AsymPol-TEKs as efficient polarizing agents for MAS-DNP in glass matrices of non-aqueous solvents

Rania Harrabi[a], Thomas Halbritter[b], Shadi Alarab[a], Satyaki Chatterjee[b], Malgorzata Wolska-Pietkiewicz[c], Krishna K. Damodaran[b], Johan van Tol[e], Daniel Lee[a,d], Subhradip Paul[a], Sabine Hediger[a], Snorri Th. Sigurdsson*[b], Frederic Mentink-Vigier*[e], Gaël De Paëpe*[a]

a. Univ. Grenoble Alpes, CEA, CNRS, IRIG, MEM, 38000 Grenoble (France)
b. University of Iceland, Department of Chemistry, Science Institute, Dunhaga 3, 107 Reykjavik (Iceland)
c. Faculty of Chemistry, Warsaw University of Technology, Noakowskiego 3, 00-664 Warsaw (Poland)
d. Current address: Department of Chemical Engineering, University of Manchester, Manchester, M13 9PL, UK
e. National High Magnetic Field Laboratory, Florida State University, Tallahassee, FL 32301 (USA)

Table of contents

Abbreviations

DCC   dicyclohexyl carbodiimide
DCE   1,2-dichloroethane
DNP   Dynamic Nuclear Polarization
ESI-HRMS   electron spray ionization high resolution mass spectrometry
EPR   electron paramagnetic resonance
EtOAc   ethyl acetate
Et_3N triethylamine
HOBt   1-hydroxybenzotriazol
MAS   Magic Angle Spinning
NMR   nuclear magnetic resonance
PA   polarizing agent
PMA   phosphomolybdic acid
Pet. ether   petroleum ether
Satd.   saturated
TCE   1,1,2,2-tetrachloroethane
TLC   thin layer chromatography
UV   ultra violet

General materials and methods

All commercially available reagents were purchased from Sigma-Aldrich, Inc. or Acros Organics and used without further purification. Water was purified on a Millipore Milli-Q deionizer. All moisture- and air-sensitive reactions were carried out in oven-dried glassware under an inert atmosphere of Ar. Thin-layer chromatography (TLC) was performed using glass plates pre-coated with silica gel (0.25 mm, F-25, Silicycle) and compounds were visualized under UV light or PMA staining. Column chromatography was performed using 230–400 mesh silica gel (Silicycle). Radicals show broadening and loss of NMR signals due to their paramagnetic nature and, therefore, those NMR spectra are not shown. EPR spectra were recorded on a MiniScope MS200 (Magnettech Germany) spectrometer. Mass spectrometric analyses of all organic compounds were performed on an ESI-HRMS (Bruker, MicrOTOF-Q) in a positive ion mode. HPLC analytical seperations were performed on an Agilent Pursuit 5 C18 (300 Å, 4.6 x 250 mm) column, using Agilent 1200 series instrument with UV detection at λ = 254 nm. Solvent gradients were run at 1 mL/min as follows: Solvent A, 0.1% TFA in H2O; solvent B, CH3CN; isocratic 4% B for 4 min, 26 min linear gradient to 100% B, 5 min isocratic 100% B, then a 5 min linear gradient to initial conditions.

Synthetic protocols
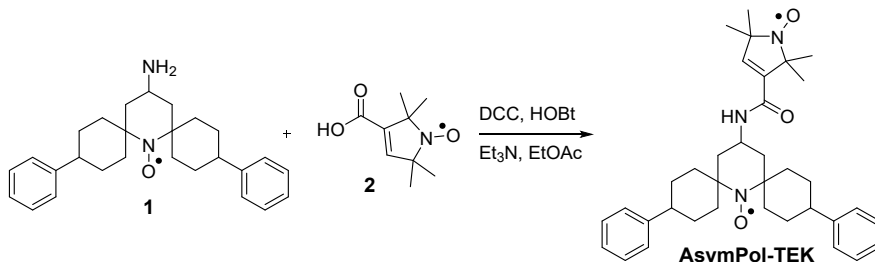
AsymPol-TEK. To a solution of nitroxide **1**[1] (0.010 g, 0.025 mmol) and nitroxide **2** (0.005 g, 0.030 mmol) in EtOAc (1.0 mL) was added DCC (0.015 g, 0.074 mmol), HOBt (0.011 g, 0.074 mmol) and Et_3N (0.014 mL, 0.099 mmol) and the resulting solution stirred at 22 °C for 24 h. 5% aq. NaOH (10 mL) was added, and the solution extracted with EtOAc (3x10 mL). The combined organic layers were washed with brine (20 mL), dried over Na_2SO_4, the solvent was removed in vacuo and the residue purified by flash column chromatography (pet. ether:EtOAc 8:2) to give **AsymPol-TEK** (0.011 g, 0.019 mmol, 77%) as an orange solid. Isomers A and B were separated on a preperative TLC (pet. ether:EtOAc 6:4, two elutions).

<u>TLC</u> (Silica gel, pet. ether:EtOAc 8:2), Rf (AsymPol-TEK, isomer A) = 0.4
(Silica gel, pet. ether:EtOAc 8:2), Rf (AsymPol-TEK, isomer B) = 0.38

<u>ESI-HRMS</u>: calcd. for $C_{36}H_{47}N_3O_3$ [M+Na$^+$] 592.3510, measured 592.3493 (Δm = 0.0017, error = 2.9 ppm).

<u>HPLC Analysis:</u>

<u>EPR</u> (DCE, 1.0 mM):
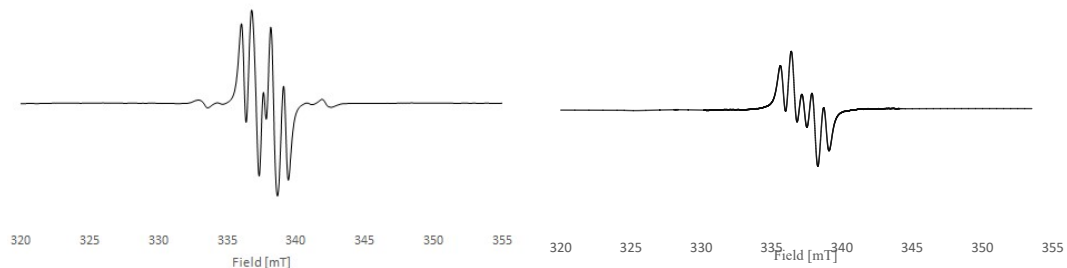
<u>X-ray crystal structure</u> (isomer A):
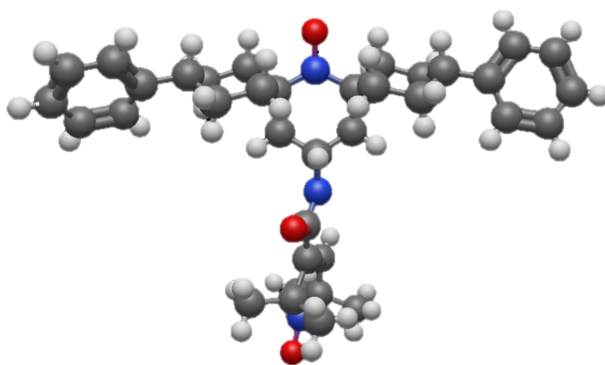
<u>Solubility tests:</u>
- 4 mg of AsymPol-TEK at 20 °C under no influence of heat or ultrasound is dissolved in 47 µL of TCE, making the maximal soluble concentration to be 150 mM. The experiment was performed three times.
- 4 mg of AsymPol-TEK at 20 °C under no influence of heat or ultrasound is dissolved in 40 µL of chloroform, making the maximal soluble concentration to be 175 mM. The experiment was performed three times.
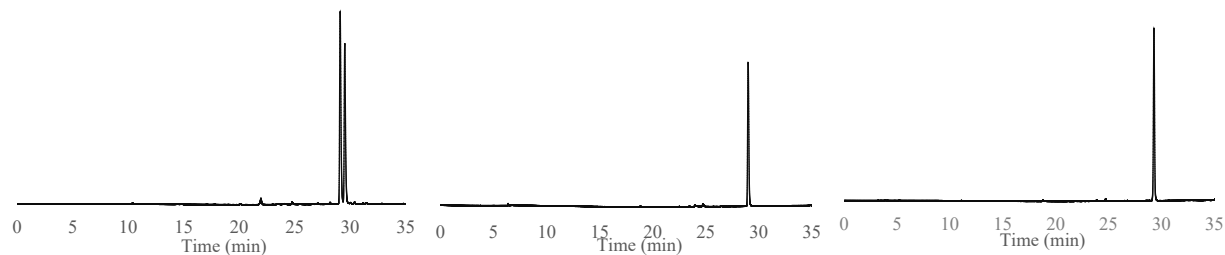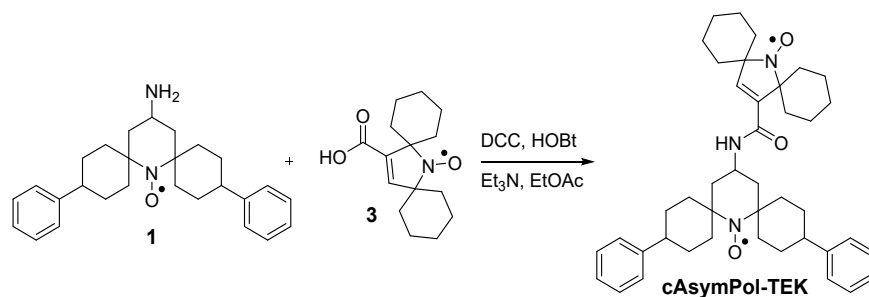
cAsymPol-TEK. To a solution of nitroxide **1**[1] (0.010 g, 0.025 mmol) and nitroxide **3** (0.008 g, 0.030 mmol) in EtOAc (1.0 mL) was added DCC (0.015 g, 0.074 mmol), HOBt (0.011 g, 0.074 mmol) and Et$_3$N (0.014 mL, 0.099 mmol) and the resulting solution was stirred at 22 °C for 24 h. 5% aq. NaOH (10 mL) was added and the solution was extracted with EtOAc (3x10 mL). The combined organic layers were washed with brine (20 mL), dried over Na$_2$SO$_4$, the solvent was removed in vacuo and the residue purified by flash column chromatography (pet. ether:EtOAc 8:2) to give **cAsymPol-TEK** (0.12 g, 0.018 mmol, 72%) as an orange solid.

TLC (Silica gel, pet. ether:EtOAc 8:2), Rf (cAsymPol-TEK) = 0.5

ESI-HRMS: calcd. for C$_{42}$H$_{55}$N$_3$O$_3$ [M+Na$^+$] 672.4136, measured 672.4131 ($^\Delta$m = 0.0005, error = 0.7 ppm).
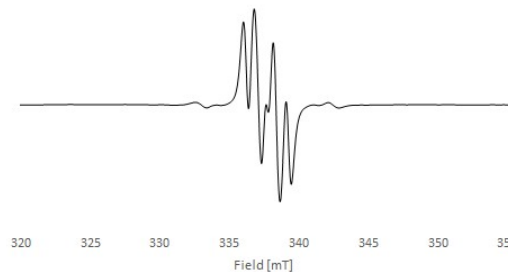
EPR (DCE, 1.0 mM):   HPLC chromatogram:
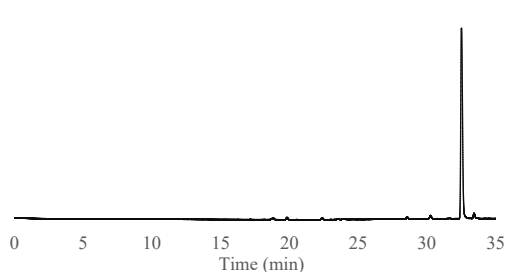
X-ray crystal structure:
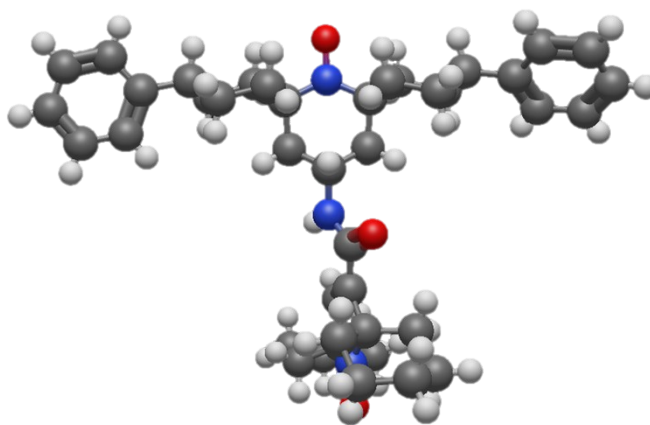
X-ray crystallography

X–ray quality single crystals of AsymPol-TEK and cAsymPol-TEK were obtained by layering n-hexane over a solution of biradical in $CHCl_3$. The crystals were isolated from the solvent, immersed in cryogenic oil and mounted on a Bruker D8VENTURE (Photon100 CMOS detector) diffractometer equipped with a Cryostream open–flow nitrogen cryostat. The data were collected using CuKα radiation (λ = 1.542 Å). The unit cell determination, data collection, data reduction, structure solution/refinement and empirical absorption correction (SADABS) were carried out using Apex-III (Bruker AXS: Madison, WI, 2015). The structure was solved by direct method and refined by full-matrix least squares on F^2 for all data using SHELXTL version 2017/1.[2] All non–hydrogen atoms were refined anisotropically and the hydrogen atoms were placed in the calculated positions and refined using a riding model. The solvent molecule in cAsymPol-TEK was found to be severely disordered, and we were not able to refine the disordered hexane molecule to a proper model and the contribution of the electron densities from the solvent molecules were excluded using PLATON/SQUEEZE.[3] The details of X-ray data are given in **Table S1** and the crystallographic data were deposited at the Cambridge Crystallographic Data Centre, and the CCDC numbers are 2279465 & 2279466. These data are provided free of charge by the joint Cambridge Crystallographic Data Centre and Fachinformationszentrum Karlsruhe.

Table S1. Crystal data

Crystal data	AsymPol-TEK	cAsymPol-TEK
Empirical formula	$C_{36}H_{47}N_3O_3$	$C_{42}H_{55}N_3O_3$
Color	Orange	Brown
Formula weight	569.76	649.89
Crystal size (mm)	0.420 x 0.115 x 0.096	0.35 x 0.13 x 0.05
Crystal system	Orthorhombic	Monoclinic
Space group	$Pna2_1$	$P2_1/c$
a (Å)	12.9895(4)	13.7437(3)
b (Å)	22.8945(6)	11.1387(3)
c (Å)	10.7431(3)	26.0109(6)
α (°)	90	90
β (°)	90	100.8430(10)
γ (°)	90	90
Volume (Å³)	3194.87(16)	3910.84(16)
Z	4	4
$D_{calc.}$ (g/cm³)	1.185	1.104
F(000)	1232	1408
μ (mm⁻¹) CuK_α	0.588	0.536
Temperature (K)	150(2)	150(2)
Reflections collected/ unique/observed [I>2σ(I)]	60273/5928/5745	80372/7991/7346
Data/restraints/parameters	5928/1/384	7991/0/433
Goodness of fit on F^2	1.025	1.042
Final R indices [I>2σ(I)]	R_1 = 0.0307 wR_2 = 0.0831	R_1 = 0.0493 wR_2 = 0.1328
R indices (all data)	R_1 = 0.0321 wR_2 = 0.0842	R_1 = 0.0525 wR_2 = 0.1359

Liquid state EPR data

Liquid state EPR spectra of AsymPol-TEK and cAsymPol-TEK in TCE at room temperature were fitted using Easyspin v5.2.23,[4–6] the method pepper, and assuming isotropic interactions. Lines were a mixture of Lorentzian and Gaussian lineshapes, with linewidtsh of 0.20 and 0.28 mT, respectively. Best fits are shown in Fig. S1.

The fits enable to extract the isotropic g_{iso} value, the hyperfine A_{iso} and the exchange $|J_{a,b}|$ interactions. For both biradicals, we obtained g_{iso} = 2.0056 and A_{iso} = 39 MHz for the five-membered ring, and g_{iso} = 2.0059 and A_{iso} = 42 MHz for the six-membered one. The absolute value of the exchange interaction was found to be $|J_{a,b}|$ = 55 MHz (see below for definition). This value has to be compared to the one of AsymPol-POK, in water, fount at $|J_{a,b}|$ = 78 MHz. This confirms the impact of the solvent on the exchange interaction. Importantly, these values may not represent the solid-state exchange interaction.
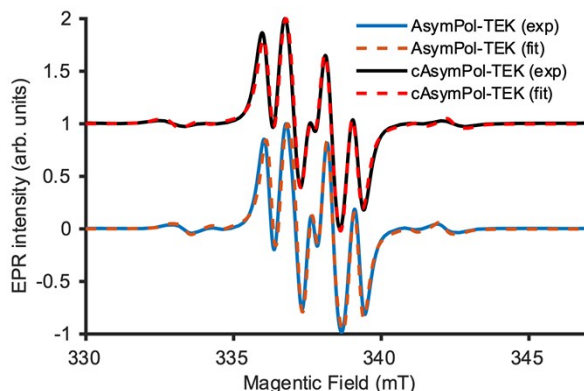
Fig. S1. Experimental and fitted EPR spectra at X-band and room temperature of AsymPol-TEK (blue and orange, respectively) and cAsymPol-TEK (black and red, respectively) in TCE.

Data analysis for MAS-DNP and solid-state NMR experiments

Evaluation of DNP enhancement factor, depolarisation and sensitivity

To characterize the MAS-DNP performance, the ^{13}C signal intensity of either the solvent TCE or the impregnated powders was measured using a ^{1}H-^{13}C CP experiment. The polarization build-up time, T_B, was obtained from proton saturation recovery experiments under µw irradiation, fitting the curve with a mono-exponential function for the homogeneous frozen solution. To determine the enhancement factor $\epsilon_{on/off}$, the ^{13}C CP-MAS spectra were recorded with (S_{on}) and without, µw irradiation (S_{off}) with the repetition delay set to $1.3 \times T_B$. The enhancement factor is then:

$$\varepsilon_{on/off} = \frac{S_{on}}{S_{off}}$$

The depolarization factor ϵ_{Depo}, was measured as previously described on the ^{1}H magnetization,[7,8] using the procedure proposed by Chen *et al.*[9] to minimize the proton background signal. This procedure requires the acquisition of a π/2-pulse and a π-pulse ^{1}H spectrum in absence of µw. They are then combined to obtain a ^{1}H spectrum with highly reduced background signal, allowing the measure of the signal intensity, S_{off}^{1H}. The procedure was repeated at different spinning frequencies with a recycle delay of 30 s at 9.4 T and 80 s at 14.1 T. ϵ_{depo} as a function of the MAS frequency ν is then obtained from the ratio:

$$\varepsilon_{depo}(\nu) = \frac{S_{off}^{1H}(\nu)}{S_{off}^{1H}(0)}$$

Lastly, the sensitivity (normalized by the sample amount) is defined as the ratio of the signal-to-noise ratio S/N and $\sqrt{T_B}$ measured at a repetition time of $1.3 \times T_B$

$$Sensitivity = \frac{\dfrac{S}{N}}{\sqrt{T_B}},$$

with to the following uncertainty:

$$\Delta Sensitivity = Sensitivity\left(\frac{\Delta\left(\dfrac{S}{N}\right)}{\dfrac{S}{N}} + \frac{\Delta T_B}{2T_B}\right).$$

Standard deviations $\Delta(S/N)$

$\Delta(S/N)$
and ΔT_B were calculated by repeating the sample preparation and the DNP measurement three times. The largest error in sensitivity turned out to be 10%, which was then applied to all the data series presented in the manuscript. The error estimation on $\epsilon_{on/off}$ was carried out in a similar way and found to be around 5%.

MAS-DNP efficiency and reproducibility of the measurement

Table S2. Experimental and simulated depolarization factor εdepo for TEKPol, AsymPol-TEK and cAsymPol-TEK in TCE at 9.4 T and 14.1 T (8 kHz MAS and 105 K).

9.4 T	$\mathcal{E}_{depo}$[b]
TEKPol (16 mM)	0.5 ± 0.05 / **0.5**
AsymPol-TEK (16 mM)	0.8 ± 0.05 / **0.73**
cAsymPol-TEK (16 mM)	0.9 ± 0.05 / **0.67**
14.1 T	
TEKPol (10 mM)	0.6 ± 0.05 / **0.52**
TEKPol (16 mM)	0.52 ± 0.05 / **0.52**
AsymPol-TEK (10 mM)	0.75 ± 0.05 / **0.75**
cAsymPol-TEK (10 mM)	0.75 ± 0.05 / **0.65**

[a] Light and bold numbers are experimental and simulated values, respectively.

DNP build-up analysis

The ^{1}H build-up time (T_B) was measured through saturation-recovery ^{1}H-^{13}C CPMAS experiments. For homogenous systems, such as the radical frozen solutions, the resulting build-up curves $S(T)$ can be fitted as a mono-exponential function. For heterogeneous systems, such as the organic microcrystals, a one-component fit is often not good enough to reproduce the data. In the examples reported herein, we used a two-component build-up function to improve the quality of the fit:

$$S(T) = S_0 \left[\frac{A_1}{A_1 + A_2} \left(1 - e^{-\left(\frac{T}{T_{B1}}\right)} \right) + \frac{A_2}{A_1 + A_2} \left(1 - e^{-\left(\frac{T}{T_{B2}}\right)} \right) \right]$$

Where S_0 is the signal integral of the ^{13}C resonances, T_{B1} and T_{B2} are the short and the long component of the build-up function, respectively, with $A_1/(A_1 + A_2)$ and $A_2/(A_1 + A_2)$ their corresponding weights. t is the incremented recycle delay in seconds. The optimum recycle delay, denoted T_{opt}, is the specific time, which maximizes the sensitivity expressed as:

$$Sensitivity(t) = \frac{S(t)}{\sqrt{t}},$$

and can conveniently be used to compare radicals. Please note that in cases of multi-exponential build-up times under microvawes, $\varepsilon_{on/off}$ depends on the recycle delay.

Table S3: Fited parameters for the ^{13}C CPMAS build-up experiments of adenosine and caffeine impregnated with 10 mM cAsymPol-TEK, AsymPol-TEK or TEKPol solutions in TCE.

	Adenosine					Caffeine				
Radical	T_{B1}	$\frac{A_1}{A_1 + A_2}$	T_{B2}	$\frac{A_2}{A_1 + A_2}$	T_{opt}	T_{B1}	$\frac{A_1}{A_1 + A_2}$	T_{B2}	$\frac{A_2}{A_1 + A_2}$	T_{opt}
cAsymPol-TEK	10 s	38%	140 s	62%	16 s	2.9 s	100%	-	-	3.6 s
AsymPol-TEK	10 s	35%	136 s	65%	17 s	4 s	100%	-	-	5 s
TEKPol	27 s	30%	250 s	70%	40 s	4 s	100%	-	-	5 s

Polarizing proton-dense molecular solids

SR26 MAS-DNP NMR experiments

The ^{13}C-^{13}C DQ-SQ dipolar correlation spectra of Figure 8 and S2 using the SR26 recoupling sequence[10,11] combined with StiC phase shifts,[12] were acquired at 9.4 T and 6.6 kHz MAS frequency. For the SR26 recoupling periods, the ^{13}C RF-field strength was set to 42.9 kHz and a continuous-wave Lee-Goldburg (CW-LG) decoupling[13] was applied on the proton channel at an RF-field strength of 100 kHz. 100 kHz SPINAL-64 ^{1}H decoupling[14] was applied during the direct and indirect acquisition periods of 20 and 3.2 ms, respectively, for the adenosine sample, and 20 ms and 2.8 ms, respectively, for the caffeine sample. For the adenosine sample, 16 transients were acquired for each of the 128 points of the indirect dimension using STATES-TPPI[16] quadrature detection, with a recycle delay of 18 s for a total experimental time of ⌣ 10 h. For the caffeine sample, 32 transients were acquired for each of the 64 points of the indirect dimension using STATES-TPPI with a recycle delay of 2 s for a total experimental time of ⌣ 1.16 h. Prior to Fourier transform, data were zero-filled and apodized with 50 Hz exponential line broadening in both dimensions.

For the Histidine.H$_2$O.HCl, the DQ excitation and reconversion were set to 500 µs. SPINAL-64 ^{1}H decoupling[14] was applied during the direct and indirect acquisition periods of 17 ms, 32 transients were acquired for each of the 100 points of the indirect dimension using STATES- TPPI quadrature detection, with a recycle delay of 30 s for a total experimental time of ⌣ 26 h.
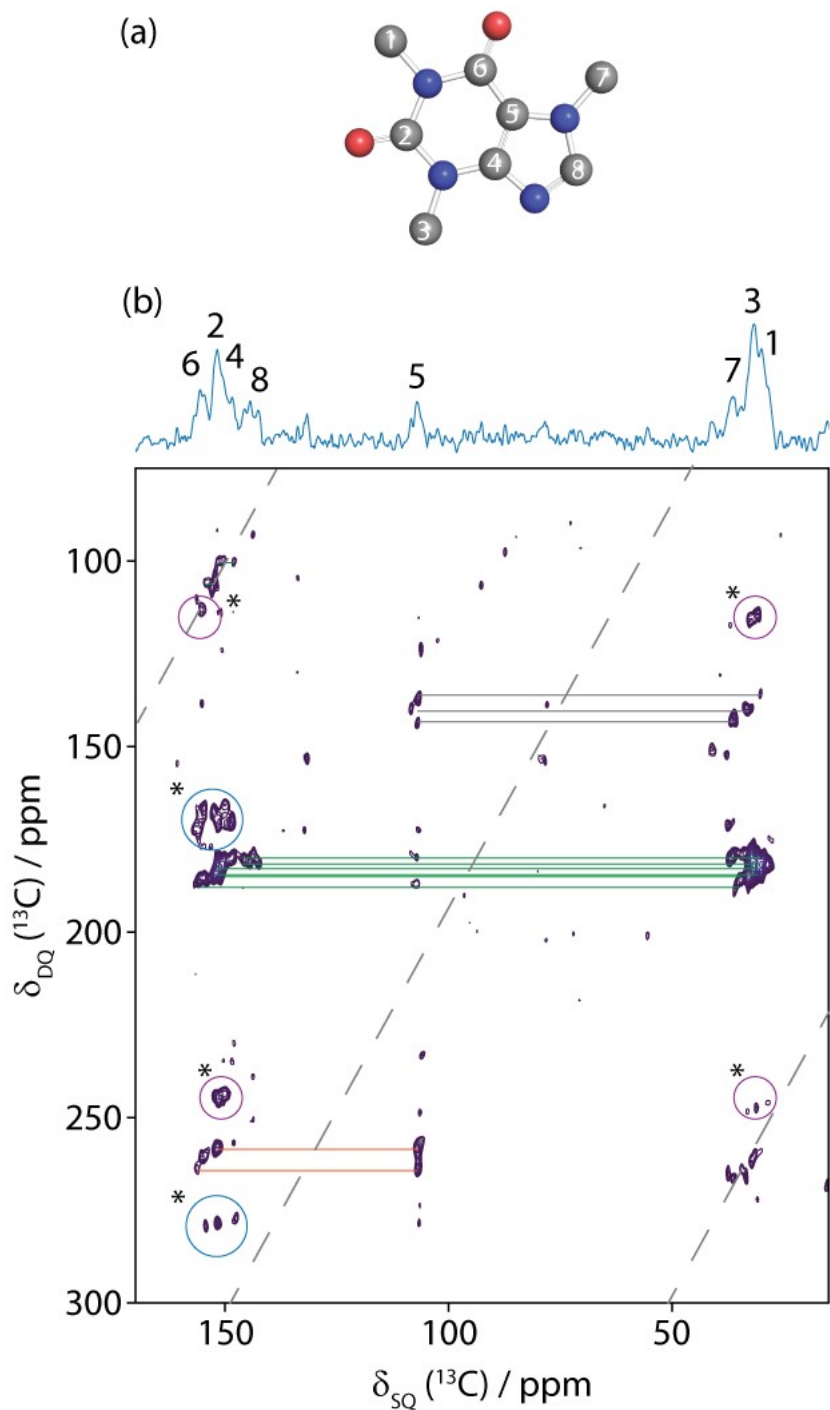
Fig. S2. (a) Structure and (b) DNP-enhanced 2D ^{13}C-^{13}C DQ-SQ correlation spectra of caffeine microcrystals at NA using cAsymPol-TEK. The experiment was acquired using SR26 as dipolar recoupling sequence, at 6.6 kHz MAS, 105 K and 9.4 T. Experimental time was 1.16 h and the total mixing time for SR26 was 4.8 ms. ^{13}C-^{13}C correlations are mapped out in the 2D spectra, in orange for one-bond correlactions, green for two-bonds, and grey for ≥ three-bonds. Peaks corresponding to spinning side bands (purple circles) and folded spinning sidebands (blue circles) are indicated with asterisks.
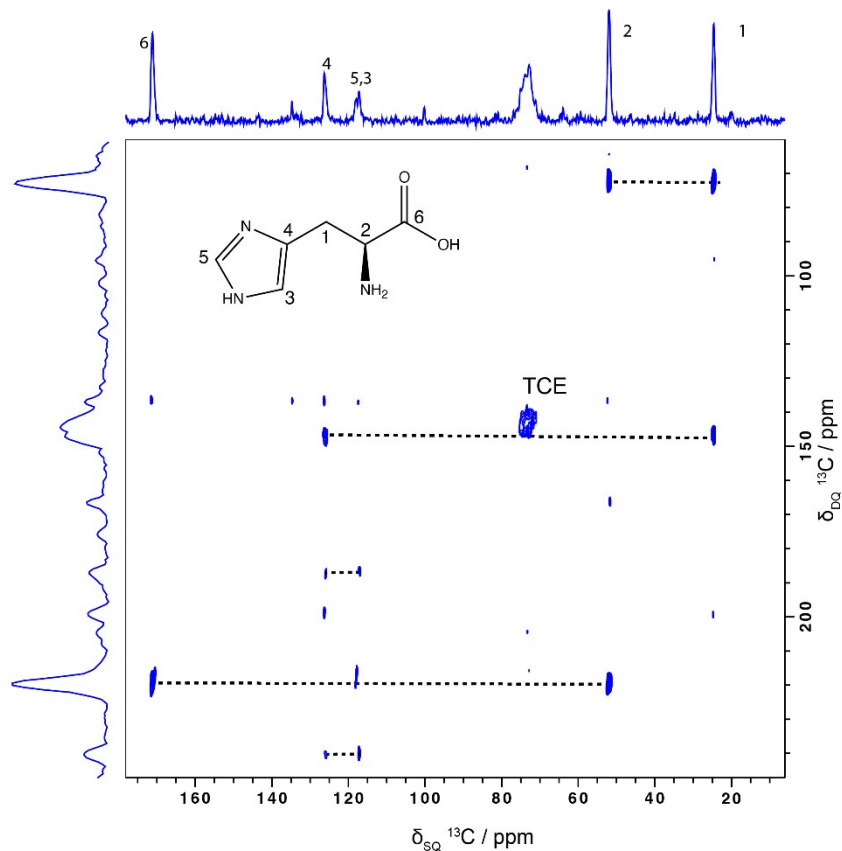
Fig. S3. (a) Chemical structure and DNP-enhanced 2D ^{13}C-^{13}C DQ-SQ correlation spectra of Histidine.H_2O.HCl at NA using 10 mM AsymPol-TEK. The experiment was acquired using R26 as dipolar recoupling sequence, at 8 kHz MAS, 100 K and 14.1 T. Experimental time was 20 h. ^{13}C-^{13}C correlactions are mapped out in the 2D spectra, in black dotted line for one-bond correlactions.

ZnO nanocrystals coated by diphenyl phosphate ligands

Synthesis

ZnO NCs were synthesized according to the recently described OSSOM procedure.[15,16] ZnEt$_2$ in hexane (1 mL of a 2 M solution in hexane, 2 mmol) was added to a stirred solution of 2.0 mmol of diphenyl phosphate (500 mg) in THF (15 mL) at −78°C by using inert atmospheric Schlenk technique, and then the reaction mixture was allowed to warm to room temperature and stirred for 3 h. In the second step, a solution of the resulting ethylzinc precursor in THF was exposed to air to initiate transformations and stirred for 5 days at ambient conditions. Subsequently, the liquid residual was evaporated in vacuo. Then, the ZnO-DPP NCs were redispersed in THF and were precipitated using hexane, centrifuged, and rewashed with hexane. The as-prepared ZnO NCs were dried under vacuum.

MAS-DNP simulations

Definition and notations

The nuclear polarization at thermal equilibrium, in the presence and absence of µw irradiation, are defined as $P_{n,Boltzman}$, $P_{n,on}$, and $P_{n,off}$, respectively. The resulting polarization gain ϵ_B and the depolarization ϵ_{depo} are defined as:

$$\epsilon_B = P_{n,on}/P_{n,Boltzman}$$

$$\epsilon_{depo} = P_{n,off}/P_{n,Boltzman}$$

Experimentally, the ratio $\epsilon_{on/off}$ corresponds to the ratio of the NMR signal in presence and absence of ⸕w irradiation:

$$\epsilon_{on/off} = S_{on}/S_{off} = P_{n,on}/P_{n,off}$$

This last ratio is routinely reported when quantifying the efficiency of nitroxide biradicals, although it has been demonstrated in general that $\epsilon_B \neq \epsilon_{on/off}$.[7,17,18]

The distance between the g-tensors, $L_{a,b}$, is an essential parameter for the CE mechanism.[19] It correlates the polarization performance with the relative orientation of the two nitroxide g-tensors. For two tensors, a and b, with respective Euler angles (0,0,0) and $\Omega = (\alpha,\beta,\gamma)$, $L_{a,b}$ is defined as the Frœbenius norm of the tensor difference:

$$L_{a,b}(\Omega) = \|(\hat{g}_a - \hat{g}_b(\Omega))\|_{Fro} = \sqrt{Tr\left[(\hat{g}_a - \hat{g}_b(\Omega))^{\dagger}(\hat{g}_a - \hat{g}_b(\Omega))\right]}.$$

Where $\hat{g}_a$ and $\hat{g}_b(\Omega)$ represents the g tensors matrices for the relative orientation $\Omega = (\alpha,\beta,\gamma)$. The norm accounts for both the effect of the relative orientation and the anisotropy of the g-tensors, and is a natural quantity for defining how two g-tensors relate. The trivial case $L_{a,b}(0,0,0) = 0$ only generates SE.[20,21] Except otherwise specified, all angles are in degrees.

The MAS-DNP simulations were carried out as in refs. [8,18,22,23]. In the µw rotating frame, the time-dependent Hamiltonian can be written as:

$$\hat{H}(t) = \hat{H}_Z(t) + \hat{H}_{HF}(t) + \hat{H}_D(t) + \hat{H}_J + \hat{H}_d + \hat{H}_{\mu w} = \hat{H}_0(t) + \hat{H}_{\mu w}$$

where

$$\hat{H}_Z(t) = \sum_n \sum_i (g_i(t)\beta_e B_0 - \omega_{\mu w})\hat{S}_{z,i} + m_{I,i}A^N_{z,i}(t)\hat{S}_{z,i} - \omega_n\hat{I}_{z,n}$$

$$\hat{H}_{HF}(t) = \sum_i \left\{ A_{z,i,n}(t)\hat{S}_{z,i}\hat{I}_{z,n} + 2\left(A^+_{i,n}(t)\hat{S}_{z,i}\hat{I}^+_n + A^-_{i,n}(t)\hat{S}_{z,i}\hat{I}^-_n\right)\right\}$$

$$\hat{H}_D(t) = \sum_{a<b} D_{a,b}(t)\left(2\hat{S}_{z,a}\hat{S}_{z,b} - \frac{1}{2}(\hat{S}^+_a\hat{S}^-_b + \hat{S}^-_a\hat{S}^+_b)\right)$$

$$\hat{H}_J = \sum_{a<b} -2J_{a,b}\left(\hat{S}_{z,a}\hat{S}_{z,b} + \frac{1}{2}(\hat{S}^+_a\hat{S}^-_b + \hat{S}^-_a\hat{S}^+_b)\right)$$

$$\hat{H}_d(t) = \sum_{i,j} d_{i,j}(t)\left(2\hat{I}_{z,i}\hat{I}_{z,j} - \frac{1}{2}(\hat{I}^+_i\hat{I}^-_j + \hat{I}^-_i\hat{I}^+_j)\right)$$

$$\hat{H}_{\mu w} = \sum_i \omega_{1,s}\hat{S}_{x,i}$$

g_i is the g-tensor value for electron i, $\omega_{\mu w}$ the µw irradiation frequency, $A^N_{z,i}$ the secular part of the hyperfine interaction between electron i and ^{14}N that bears the radical, ω_n the nuclear Larmor frequency, $A_{i,n}$ the hyperfine coupling between electron i and nucleus n, $D_{a,b}$ the dipolar coupling between electrons a and b, and $J_{a,b}$ the exchange interaction between electrons a and b (the two radical moieties, respectively), $d_{n,n'}$ is

the dipolar coupling between nuclei n and n'. The µw Rabi frequency, $\omega_1/2\pi$, is assumed to be small and is treated as a perturbation. Evolution superoperators were calculated as described in detail in ref.21 The nuclear polarization enhancements were then calculated as

$$\epsilon(Nt_r) = \frac{Tr(\rho(Nt_r)\hat{I}_z)}{Tr(\rho(0)\hat{I}_z)}$$

Parameters used in the simulations

Except otherwise specified, the experimental parameters considered for the simulations were:
- Magnetic field: 9.3973 T / 14.0959 T
- µw frequency: 263.45 GHz / 395.175 GHz
- Temperature: 100 K
- µw nutation frequency: 0.5 MHz @ 9.4 T and 0.3 MHz @14.1 T
- µw irradiation duration: 40 s
- MAS frequency: 8 kHz

For both models, the spin parameters were:
- Electron relaxation is assumed anisotropic $T_{1,e} = f(g) \times T_{1,e}^{min}$, where g is the effective g-value. The function f is a 2nd degree polynomial obtained from the fit of the data measured in ref [18].
- For the five-membered ring with methyl groups in alpha of the N-O function, $T_{1,e}^{min} = 0.1$ ms.
- For the five-membered ring with rings in alpha of the N-O function: $T_{1,e}^{min} = 0.15$ ms.
- For the six-membered ring: $T_{1,e}^{min} = 0.2$ ms; $T_{2,e} = 2.5$ µs.
- The powder averaging was achieved using 600 three-angles REPULSION crystal orientations.[24]

Specific parameters used for the "Box model" simulations
- Principle Axis Frame (PAF) ^{1}H hyperfine coupling: [3 3 -6] MHz, connected to the five-membered ring nitroxide with relative orientation with respect to electron a's g-tensor [θ,ϕ]=[60,30] degrees (box model)
- For located ^{1}H having a dipolar hyperfine coupling with Principle Axis Frame (PAF) values [3 3 -6] MHz: $T_{1,n}^{3MHz} = 0.04$ s at 9.4 T and 0.1 s at 14.1 T.
- Biradical concentration: 10 or 16 mM
- Interaction between radicals is considered if the distance is shorter than 8 nm (0.1 MHz)
- Each box contained 60 randomly distributed biradicals.
- The minimal distance between two nitroxides of different molecules was set to 1.8 nm.

Specific parameters used for the "Multi-nuclei" model simulations
- The hyperfine couplings, isotropic and anisotropic, of the protons on the biradicals were extracted from DFT simulations.[8,23]
- Bulk nuclei are assumed to have hyperfine coupling values < 50 kHz
- For each biradical concentration, the number of TCE molecules was adapted to match the the biradical concentration, assuming a spherical distribution around the biradical.
- For simulations using the "multi-nuclei" model, we used our previously described model for the nuclear relaxation time.[8,18,22,23] The relaxation rate for the nuclear spin i is expressed as the sum of "hyperfine induced" relaxation rates that depends on the dipolar hyperfine couplings with the electron spin j, $A_{i,j}^{dip}$, and of other bulk relaxation mechanisms. Assuming that the electron spins generate uncorrelated relaxation mechanisms we obtain:

$$\frac{1}{T_{1,n}} = \frac{1}{T_{1,n}^{bulk}} + \frac{1}{T_{1,n}^{3MHz}} \times \left(\sum_j \left(\frac{A_{i,j}^{dip}}{3\ MHz} \right)^2 \right)$$

- The bulk nuclear relaxation time $T_{1,n}^{bulk}$ was set to 60 s, as measured on the undoped sample at 9.4 T. We assumed that the relaxation time $T_{1,n}^{3MHz}$ of nuclear spins with a dipolar hyperfine coupling of 3

MHz was 0.04 s for simulations at 9.4 T[23] and 0.1 s for simulations at 14.1 T. The 0.1 s value was chosen to improve the agreement with the experimental values of the predicted build-up times of TEKPol.

Table S4: MAS-DNP Simulations of 10 mM cAsymPol-TEK, AsymPol-TEK and TEKPol in TCE, at 9.4 T and 14.1 T, 8 kHz MAS and 105 K.

	R_B^{Box}	R_{Depo}^{Box}	$R_{on/off}^{Box}$	$\varepsilon_B^{multi-nuclei}$	$\varepsilon_{Depo}^{multi-nuclei}$	ε_B^{sim}	ε_{Depo}^{sim}	$\varepsilon_{on/off}^{sim}$
Biradical concentration of 16 mM, 9.4 T								
cAsymPol-TEK #1	83/99	0.68/0.79	1	44	0.9	36.9	0.77	48
cAsymPol-TEK #2	198/252	0.48/0.62	1	180	0.65	141.4	0.50	281
AsymPol-TEK #1	66/73	0.73/0.8	1	43	0.92	38.9	0.85	46
AsymPol-TEK #2	179/223	0.52/0.64	1.05	178	0.69	146.1	0.56	261
TEKPol	121/239	0.39/0.58	303/410	183	0.64	114.8	0.51	226
Biadical concentration of 10 mM (except explicitly mentioned), 14.1 T								
cAsymPol-TEK #1	28/35	0.62/0.73	50/57	19	0.85	15.9	0.77	21
cAsymPol-TEK #2	101/149	0.4/0.56	1	105	0.57	81.2	0.45	181
AsymPol-TEK #1	14/15	0.76/0.8	1	12	0.95	10.8	0.91	12
AsymPol-TEK #2	92/127	0.42/0.57	1	100	0.63	77.3	0.50	156
TEKPol	69/110	0.46/0.58	151/191	95	0.65	59.6	0.52	116
TEKPol (16 mM)	60/112	0.42/0.57	136/190	105	0.59	54.4	0.45	120

DFT simulations, xyz files

AsymPol-TEK conformer #1

89
AsymPol-TEK conf 1

```
 N  -0.47799383506794   -3.71824761737154   -3.82587159643231
 C  -0.37744148441591   -4.21129818577041   -2.41193732496892
 C  -0.21198505931017   -2.30310499551757   -4.25898118624263
 C  -0.78809457456436   -3.09840872153169   -1.44603165259249
 C  -0.61050740596584   -1.31976460143342   -3.15115863461589
 C  -0.13916140465166   -1.75862796824996   -1.77571169657409
 N  -0.49164704299878   -0.75037827403501   -0.78027392875505
 C  -1.06694640761593   -2.04168142755713   -5.51429396228829
 C   1.28283501640180   -2.17705785193846   -4.63920786565723
 C   1.06501261719010   -4.70548206740630   -2.15458121657302
 C  -1.33772714889754   -5.40712757854603   -2.27014409273505
 O  -0.36669246826132   -4.60985453975333   -4.73942465868315
 C  -1.03259344796002    1.43946875324425    1.08290100310123
 C  -1.45650500531455    2.21642889145049    2.29305762243831
 C  -0.39750998755105    0.30225642340345    1.38510284268919
 N  -1.02140826339459    1.28613650488070    3.36507778496968
 C  -0.24204434323044    0.11294801572703    2.87927532016775
 O  -1.15350008617189    1.55561879063274    4.59926701054620
 C  -0.72379422558149    3.55797766985691    2.42102219200288
```

13

```
C   1.20795734542531     0.23398705821769     3.36522871008554
H  -1.87951501580377    -2.97162807629471    -1.48298642487795
H  -0.52973389085407    -3.39044552659089    -0.42489842375264
H  -0.20671019196543    -0.33149217475747    -3.39004850009609
H  -1.70643922714590    -1.22687377548383    -3.13451815709309
H   0.95255702258023    -1.85124472700144    -1.75089411914522
C   0.13300491158032    -0.70017753666638     0.42456402591023
O   1.08913961770444    -1.42974151053375     0.71038961139422
C  -0.88310322288909    -1.18216258712081     3.38422775136691
H  -1.38400950584009    -0.28614904176330    -0.87573784413543
H   1.67237775716427     1.14374618862655     2.97244698283937
H   1.78334188023543    -0.63029008911263     3.02909685937678
H   1.21476643189960     0.27409452598641     4.45923743203448
H  -0.31346619116467    -2.03994546522893     3.01579275958723
H  -1.91842326701513    -1.26491006229546     3.03859424779814
H  -0.87136348300916    -1.19540147091378     4.47830565686346
C  -2.97502366119717     2.41657394316398     2.35540590303520
H   0.36003335405945     3.41376903830411     2.38414508516490
H  -0.98913356956920     4.03189950967202     3.37100930596417
H  -1.02027754184133     4.22148791499396     1.60275170431418
H  -3.29672237112089     3.07450805948016     1.54225868800727
H  -3.24508102361851     2.88112404564950     3.30877430531334
H  -3.49582757300588     1.45857711150339     2.26539255337551
H  -1.09496535058540    -6.13661326370730    -3.04956164537735
H  -2.36553850574428    -5.06456920905733    -2.44596861705004
C  -1.22090736325131    -6.07770890606520    -0.90154633034714
H   1.32002882382373    -5.39787696239673    -2.96691764018869
C   1.21371129228152    -5.41488069375945    -0.80635393713290
H   1.77398461555788    -3.87191814601351    -2.20277150161972
H  -0.86710984792557    -2.83932603461272    -6.23692940388564
C  -0.75332850463950    -0.69267223072477    -6.16165136751201
H  -2.12830777790197    -2.10201153531833    -5.24160955617148
H   1.51430220064353    -3.00921905861014    -5.31577953380062
H   1.91686319495530    -2.29432701654266    -3.75355193939328
C   1.61650913483211    -0.85261070168241    -5.33012547503417
C   0.72882518235832    -0.60329304649019    -6.55874540354147
H   2.67056379110713    -0.86495606660064    -5.63456094930546
H   1.51142383211267    -0.01627580135049    -4.62663689471318
H   0.92463221069132    -1.41343836142356    -7.27752157512220
C   1.06000120704353     0.70392900164648    -7.24087221575666
H  -1.00403153797034     0.13364308259164    -5.48341001374712
H  -1.38004846784976    -0.56560947115528    -7.05284761449105
C   0.21327184823289    -6.56967528185992    -0.64296419688903
H   1.08811251661085    -4.69689024465865     0.01429449255344
H   2.23600599694688    -5.80328994726045    -0.71728545971197
```

```
H  -1.91072235706515    -6.92950684289840    -0.85608421316782
H  -1.52531346027250    -5.38884571152625    -0.10304756996012
C   0.34173689744985    -7.24199681019796     0.70427687208585
H   0.44522386951894    -7.31914111385333    -1.41490771044119
H  -1.23220993876398     1.81391997144939     0.08288700047272
C   0.90572838799147     1.92642198823306    -6.57592713276278
C   1.52910907401500     0.72083195966999    -8.55683653523673
C   1.83686206294244     1.92132525343534    -9.19461854478072
C   1.21206195051287     3.12731228965107    -7.20890147421170
C   1.67930716141358     3.12988765674324    -8.52222896535456
H   1.65503649374518    -0.22013266414568    -9.08826847884506
H   0.54218994480379     1.94314008678745    -5.55101254715976
H   1.08563291701585     4.06568182486874    -6.67530967179828
H   2.20035582356319     1.91079108883256   -10.21876425490791
H   1.91846436327170     4.06749941347355    -9.01628533509583
C   0.11801642736780    -6.52971577856526     1.88893943394899
C   0.22887176654490    -7.15238016915687     3.12822790339340
C   0.56677863668383    -8.50256609529356     3.20829059635924
C   0.68009516690766    -8.59414826181308     0.79864172130882
C   0.79222518591676    -9.22183641595644     2.03814098628903
H   1.05676668657372   -10.27479945327004     2.08791051432814
H  -0.14686942289815    -5.47559736863771     1.84479562281885
H   0.05135223450741    -6.58175968246730     4.03602476847238
H   0.65373234718665    -8.98866091819347     4.17604814154753
H   0.85788526249047    -9.16272092403641    -0.11183842219225
```

AsymPol-TEK conformer #2

```
89
AsymPol-TEK conf 2
 N  -2.58840534015821    -2.95761448397437    -5.10158312827832
 C  -3.15276690357117    -3.68025294513987    -3.90972588831675
 C  -1.40585017099227    -2.03131799200378    -5.05953982942179
 C  -2.97316929173862    -2.83921019116945    -2.63975915972458
 C  -1.37746193115875    -1.29249895189079    -3.71966666441083
 C  -1.59001852447911    -2.22191714457741    -2.52940620665248
 N  -1.47417947231325    -1.49503920233596    -1.26898781555879
 C  -1.57464626556895    -1.02073738797916    -6.20958115886474
 C  -0.11979114076915    -2.85462052820034    -5.30343674988128
 C  -2.46065913060621    -5.05948665677220    -3.79832310631499
 C  -4.65470147139427    -3.89680262896189    -4.17844363858172
 O  -2.84939298534540    -3.48077680667354    -6.24164679926344
 C  -1.20339848666405     0.62372037177247     0.75416346568865
 C  -0.96630398622766     1.30490901038774     2.06867720440290
 C  -0.31350571026581    -0.33949595377817     0.49428340698706
 N   0.17240810575245     0.49806914575725     2.57736824571316
 C   0.72631703607244    -0.46858269789248     1.58692464447201
 O   0.74938205939235     0.75043326339746     3.68049090886268
```

```
C  -0.54985294181331    2.77274503064407    1.90668681335164
C   2.12683600937926   -0.01005523917510    1.16135412760277
H  -3.71869016058709   -2.03036634186630   -2.63910141019256
H  -3.17705420289617   -3.46531709099733   -1.76570232805277
H  -0.42422177144604   -0.76799481023883   -3.61225914560574
H  -2.17188532847157   -0.53318566840356   -3.70951165616788
H  -0.81686076140064   -2.99963078756204   -2.51855952104489
C  -0.27187585444592   -1.19423654906483   -0.72194157214797
O   0.79539828631652   -1.60726653339053   -1.19062626952627
C   0.77005616962335   -1.87074264914260    2.19806358474926
H  -2.31466772857713   -1.14517767217635   -0.83239258377665
H   2.08421189365895    0.97460482066242    0.68590147526296
H   2.55091424523425   -0.72495313205071    0.45419770375696
H   2.76619473398433    0.04923472116429    2.04801170263654
H   1.15446032004506   -2.57996846541666    1.45946970604673
H  -0.22905223361012   -2.18847744543402    2.51241972182362
H   1.43423229397923   -1.87467249431870    3.06765999379683
C  -2.16343981154921    1.18090329018144    3.01719218052720
H   0.31004867443861    2.86179244594446    1.23639213158119
H  -0.28614769896514    3.18962921184004    2.88361487693963
H  -1.38247664376810    3.34968244360379    1.49231466886535
H  -3.00998505232894    1.75032237256122    2.62115022665272
H  -1.89825645075216    1.58606206649720    3.99860667916186
H  -2.46138709490944    0.13437853128878    3.13185587826767
H  -4.76207426979416   -4.36916015926231   -5.16016797167242
H  -5.15254052897640   -2.91989546208793   -4.22648299809529
C  -5.31304577767748   -4.78544521087005   -3.12331705647175
H  -2.50130553101318   -5.52179630005383   -4.79259120516068
C  -3.12939753987975   -5.98650297177778   -2.77993780631512
H  -1.40268363809656   -4.93947566705804   -3.54028941878545
H  -1.73288429713693   -1.57922354191872   -7.13775368011812
C  -0.35068020450494   -0.11914049929547   -6.37213967223666
H  -2.47561411351360   -0.42104617798782   -6.02772363827436
H  -0.29096019336754   -3.46401361710878   -6.19985832564173
H   0.06259456603694   -3.54268275217674   -4.47103331785556
C   1.11683923886204   -1.97641440201840   -5.50978243566793
C   0.91584505867929   -0.95018853088392   -6.63495934176985
H   1.97432215712057   -2.61784520611736   -5.74886756781706
H   1.37401642926874   -1.45703186669291   -4.57760391572634
H   0.75182550951889   -1.51035398568979   -7.56812013122836
C   2.13577152254362   -0.08021387233073   -6.83053670737233
H  -0.20384675356940    0.50423414172120   -5.48071494479461
H  -0.51773132176508    0.56827433630221   -7.21050261932771
C  -4.63014830782849   -6.16059104646883   -3.05755028666992
H  -2.98712251555228   -5.60349909000299   -1.76089981794164
H  -2.63417348437697   -6.96516219048057   -2.81032639899064
H  -6.37372984387357   -4.91449974766397   -3.37169029181846
H  -5.28020404997914   -4.30986691137363   -2.13410283865699
C  -5.29203016065485   -7.07685056105218   -2.05445448590134
```

```
H  -4.73069340823835    -6.62465889187220    -4.05049631098583
C   2.60756088786366     0.74377979480510    -5.80149362174527
C   2.82190214655706    -0.07794497667452    -8.04763212572230
C   3.73117307581925     1.54368079353040    -5.98589341450848
C   4.40693263746134     1.53605658584144    -7.20527179987816
C   3.94779671426726     0.72165980484155    -8.23652300601484
H   2.09354898794716     0.76077723008498    -4.84308422052076
H   4.08211774452187     2.17532534292785    -5.17402760125024
H   5.28479893041832     2.15992851311118    -7.34862089230376
H   2.46919777929940    -0.71275919526341    -8.85784330357125
H   4.46657530144727     0.70655153469164    -9.19140919338758
C  -5.88652442604512    -8.27223304845326    -2.46663594576234
C  -5.33203000747465    -6.75155066863566    -0.69319906340216
C  -6.50524071196894    -9.12074954687256    -1.55022028168767
C  -5.94884903649403    -7.59575654101536     0.22515978457202
C  -6.53890885152309    -8.78509015472590    -0.19982462036156
H  -4.87677247529339    -5.82768092448980    -0.34368093023470
H  -5.86490135381501    -8.54081745947083    -3.52074471185652
H  -6.96166117505451   -10.04537354049459    -1.89355832004945
H  -5.96940538709031    -7.32460781285840     1.27745570031806
H  -7.02054890134005    -9.44400735766224     0.51727596169976
H  -2.02120570283774     0.92905353588853     0.10725007559859
```

cAsymPol-TEK conformer #1

103

cAsymPol-TEK conf 1
```
N  -0.50568387708416    -3.67221297245331    -3.82739117122275
C  -0.37010790241820    -4.12835892159913    -2.40403705154881
C  -0.23516496775916    -2.26947262278906    -4.30178206263776
C  -0.76611934501692    -2.99057803752590    -1.46327095190700
C  -0.60440439370604    -1.25338344101545    -3.21254809094582
C  -0.11703112416952    -1.66177693502152    -1.83357981830703
N  -0.46011644027254    -0.63590021566467    -0.85202845448590
C  -1.11242780225634    -2.03213705552772    -5.54669134007588
C   1.25358241105248    -2.16860567387282    -4.71281515782582
C   1.07934663068552    -4.60894112973384    -2.16299553797462
C  -1.31989425089918    -5.32389168433025    -2.20434546691017
O  -0.42110664108602    -4.58795826233077    -4.71960762838236
C  -0.95958724397386     1.56068832073246     1.01516371980778
C  -1.50156261935268     2.28162171138288     2.21004858265345
C  -0.41623452843780     0.37977150967837     1.32591898081672
N  -1.25384720675969     1.26617588337502     3.26646432932091
C  -0.45522891270593     0.09343427361567     2.81317492782788
O  -1.57716932340509     1.47630061050990     4.48003790514331
C  -0.74254910717512     3.58364181817629     2.53681604714188
C   0.95361231253841     0.10791307492350     3.44987840977028
H  -1.85752678613075    -2.86080089921177    -1.49267508568271
```

17

```
H  -0.49851575606004    -3.25619510901227    -0.43751266200600
H  -0.19357525758804    -0.27603377389107    -3.48292522378000
H  -1.69877193432115    -1.14730852778928    -3.18057514957170
H   0.97460361091076    -1.75569004767902    -1.81924591028369
C   0.15791158875300    -0.59309286475861     0.35771568081222
O   1.12641189510395    -1.30972180005397     0.63356811349578
C  -1.18039150009196    -1.23593017072945     3.10901080792077
H  -1.36237570594972    -0.18827012897562    -0.93701827874056
H   1.38771789553209     1.10682279012534     3.31842205668204
H   1.56413229493224    -0.59257991486116     2.86921726037250
C   0.96416643810530    -0.31401671585968     4.92067955373244
H  -0.67480391006764    -2.00593580605118     2.50914971112897
H  -2.21292996201835    -1.16302590835934     2.74487494957445
C  -1.13885203943478    -1.65451274513728     4.58019982032700
C  -3.01287292985339     2.56175938153667     2.09928101429503
H   0.33353237109232     3.37436463273941     2.56564132245536
H  -1.04929993099804     3.89362141873473     3.54479931394782
C  -1.05735495971939     4.69787490359613     1.53677900406816
H  -1.08590629172810    -6.08024067274821    -2.96067042074063
H  -2.35288899206275    -4.99439024090261    -2.37461826489461
C  -1.17533065489563    -5.94103512860498    -0.81308464632817
H   1.31880967023731    -5.33052385305637    -2.95453752306609
C   1.26011450896731    -5.26412384706489    -0.79176788155009
H   1.78372713510186    -3.77614793112197    -2.25805228050279
H  -0.93848409031406    -2.85281601308221    -6.25008388717281
C  -0.79465486336634    -0.70725233941813    -6.23988945046140
H  -2.16853979192616    -2.07058824516469    -5.25065300569353
H   1.46615098703021    -3.02426670356865    -5.36589169186014
H   1.90228023817908    -2.26224483937841    -3.83517954454626
C   1.58780923231644    -0.87107354015335    -5.45260675621673
C   0.67940337310970    -0.65377106651672    -6.67182650796498
H   2.63581704785175    -0.90536116261462    -5.77571450240038
H   1.50427598346303    -0.01123956572613    -4.77509250507314
H   0.84802189280257    -1.49381678677347    -7.36266420603192
C   1.01277870085469     0.62050478823132    -7.41202484802936
H  -1.01697201722548     0.14309882489422    -5.58154491530280
H  -1.43931731759127    -0.59698888962712    -7.12050040715996
C   0.26645722459740    -6.41289675799779    -0.55706158853293
H   1.15323464489076    -4.51340533086170     0.00165718840382
H   2.28479111990833    -5.64808953961445    -0.71076925606543
H  -1.85733196252101    -6.79556244733133    -0.72322319702965
H  -1.47284926510586    -5.22371504094897    -0.03754425167995
C   0.42172670832622    -7.01725490457288     0.81946444093523
H   0.48820832829427    -7.19754618843373    -1.29629401632983
H  -1.01531405856727     1.98022969549730     0.01577769751484
```

```
C   0.90762525449715      1.86988537738519     -6.78903378741447
C   1.43161485881117      0.57844191725229     -8.74434856307894
C   1.73783367712122      1.74726220215840     -9.43884592824256
C   1.21288113581816      3.03948836805635     -7.47871205711248
C   1.62965850612016      2.98315055948105     -8.80773266361941
H   1.51842625459803     -0.38442269996392     -9.24332345169759
H   0.58360470846799      1.93317389677999     -5.75273111288719
H   1.12508360626064      3.99964207632481     -6.97706167545707
H   2.06192914033209      1.69069840434824    -10.47464570949530
H   1.86799942419663      3.89640831336543     -9.34581112691767
C   0.22105935203198     -6.24601892586527      1.97107094372593
C   0.35727940685228     -6.80506442337951      3.23777555103647
C   0.69812047042911     -8.14959816801415      3.37912431885009
C   0.76337569388950     -8.36282752569146      0.97528382150001
C   0.90085352817295     -8.92699001424658      2.24248506407736
H   1.16759612911709     -9.97602943976020      2.34016618157771
H  -0.04532187054577     -5.19523017730525      1.87975587882479
H   0.19750817048911     -6.18888298946464      4.11879380667788
H   0.80504226791413     -8.58614055770984      4.36826605373433
H   0.92376534271781     -8.97650593530114      0.09127195989401
C   0.29796227906371     -1.67838767452573      5.10311868241665
H  -1.59778428887749     -2.64650277343959      4.67769034359517
H  -1.73560183357900     -0.95884610074360      5.18073637359099
H   0.44418176197931      0.43251417605107      5.53186882633812
H   2.00492403356619     -0.34972575185146      5.26671694648973
H   0.87214288882672     -2.43952342734302      4.55272453376729
H   0.31056483780112     -1.96907730358351      6.16070182328385
C  -3.31977401669886      3.68307211050343      1.10460858070047
H  -2.77289593779057      5.74611403370433      0.72198677219205
H  -2.91281689274306      5.33302579754939      2.43334819229625
H  -3.36379854868366      2.84775468500234      3.09973932287540
H  -3.52928011915664      1.63516640864249      1.81949052758407
H  -3.04659804232216      3.36732168092650      0.08750635260164
H  -4.40071971896505      3.86802347350571      1.09406280774465
C  -2.56141727265632      4.96261494776765      1.45955908256979
H  -0.52265566110358      5.60842711431843      1.83276193007709
H  -0.68184710657371      4.42386710683415      0.54051115667444
```

cAsymPol-TEK conformer #2

103

cAsymPol-TEK conf 2

```
N  -2.58503176334333     -2.96515228417879     -5.09705295225224
C  -3.13772498432199     -3.69167810208348     -3.90188288579541
C  -1.40512111481817     -2.03539889376784     -5.06253224929990
C  -2.94755651580840     -2.85468034114884     -2.63076007373671
C  -1.37026930294245     -1.29825936212098     -3.72222563911144
```

```
C  -1.56641015507791   -2.23095196221157   -2.53173164411397
N  -1.44548191340275   -1.50409374413661   -1.27189616112756
C  -1.58388917010192   -1.02401759185941   -6.21022857687908
C  -0.11839795321265   -2.85477098457590   -5.31577603980419
C  -2.44401433243578   -5.07081494574633   -3.80039306971977
C  -4.64196526927048   -3.90764099634739   -4.15804166799489
O  -2.85327409704624   -3.48745004234858   -6.23584484687348
C  -1.20180064921012    0.64860899735223    0.68932157950653
C  -1.01455757899414    1.32896463509969    2.00886922361858
C  -0.29690652836284   -0.31011128743102    0.46668249309260
N   0.11055841724342    0.52949956214589    2.56021148919812
C   0.71129543500767   -0.43015007006165    1.59147156921808
O   0.59993711174326    0.77643036895488    3.70957343834541
C  -0.60221627116965    2.80969760127687    1.88112616329909
C   2.12345839575465    0.03197813034467    1.16346536519851
H  -3.69584629696747   -2.04843700216542   -2.61976652484579
H  -3.14048422478257   -3.48429533673014   -1.75667061815095
H  -0.41966831005297   -0.76758624360111   -3.62254941605362
H  -2.16951196941694   -0.54415878253281   -3.70372838233084
H  -0.78859953096078   -3.00421741737242   -2.52927149002941
C  -0.24126219862843   -1.17045894962075   -0.74760206091169
O   0.82514325390992   -1.55942778765737   -1.23866464380698
C   0.74894249606877   -1.86289707451575    2.16232303858039
H  -2.28586682452558   -1.17758415113011   -0.81752630101351
H   2.07351864688786    1.08801169936134    0.87098477753873
H   2.38027214654010   -0.54403971546411    0.26749307974548
C   3.18935766162265   -0.20190016846241    2.23593370163762
H   0.93300185449960   -2.53011222597703    1.30887369725075
H  -0.24235626117043   -2.10951622038071    2.56260986098614
C   1.84304230888820   -2.08997858728541    3.20819283122690
C  -2.24494048518314    1.20076775322528    2.92767922437182
H   0.24610749136523    2.88927373434472    1.19085414693110
H  -0.25777437333983    3.13478201873508    2.87199542783185
C  -1.76555868547017    3.69244218304415    1.42511066617666
C  -3.40119746533610    2.09228284467038    2.47003408778544
H  -1.92711257133012    1.49848351130692    3.93573037212326
H  -2.55189966527282    0.14864102295377    2.97383949242466
H  -4.75807186693400   -4.37657327413297   -5.14045715781439
H  -5.14008393651529   -2.93052841215050   -4.19841100221921
C  -5.29081783689498   -4.79968670592444   -3.10013285069937
H  -2.49239767445531   -5.53031209211154   -4.79561368393804
C  -3.10404695710021   -6.00121897090842   -2.77929752025913
H  -1.38405983762116   -4.95057027392785   -3.55051565204965
H  -1.74530533662149   -1.58178533079578   -7.13829819932953
C  -0.36361137184692   -0.11812674929807   -6.37775438690360
H  -2.48575680564995   -0.42746314070775   -6.02259266072334
H  -0.29303323402134   -3.46239290587247   -6.21275124128301
H   0.07042004780175   -3.54451385261531   -4.48623112086327
C   1.11460163444931   -1.97276158865665   -5.52668839598215
```

```
C   0.90448709376351    -0.94436537411277    -6.64827453554048
H   1.97242222443233    -2.61128529354609    -5.77236144100231
H   1.37582668353797    -1.45535489138354    -4.59449805692730
H   0.73793351827486    -1.50285006768196    -7.58200613172168
C   2.12083992358470    -0.07020913912780    -6.84737234742518
H  -0.21449355977294     0.50436564232569    -5.48612268450636
H  -0.53717623126501     0.56997862087626    -7.21421776054517
C  -4.60704588601169    -6.17481591297802    -3.04485095708902
H  -2.95327611945836    -5.62118788001599    -1.76037591768547
H  -2.60883543229484    -6.97962316911863    -2.81671046218854
H  -6.35369465924025    -4.92805922499631    -3.33927710578976
H  -5.24905182760212    -4.32725813709546    -2.10968309295080
C  -5.26139388286045    -7.09433371530660    -2.03989650842728
H  -4.71554049016097    -6.63536944357116    -4.03862160004559
C   2.59472724464102     0.75278256622876    -5.81847999447941
C   2.80200138443436    -0.06366468003937    -8.06723390684316
C   3.71560539203041     1.55584286210455    -6.00572105205115
C   4.38646124402232     1.55244159142566    -7.22782325829156
C   3.92514064239579     0.73913960369861    -8.25897105269829
H   2.08468197849334     0.76629866511797    -4.85789286744429
H   4.06831946225097     2.18655500561614    -5.19389703921105
H   5.26225962331702     2.17871559431498    -7.37334511740702
H   2.44763481029512    -0.69771336804671    -8.87731978577878
H   4.44008762412302     0.72734555727068    -9.21597414675666
C  -5.86380533008325    -8.28562459749266    -2.45243808123968
C  -5.28801406956850    -6.77543581604423    -0.67677503365143
C  -6.47738173379763    -9.13631334099017    -1.53458914669587
C  -5.89964112971941    -7.62186571857460     0.24300053991583
C  -6.49782494521245    -8.80699408462308    -0.18237908385499
H  -4.82647644086329    -5.85478761388563    -0.32697577736915
H  -5.85275954531335    -8.54911631597241    -3.50799290113610
H  -6.94026687903256   -10.05759374583463    -1.87826354753213
H  -5.90986873602525    -7.35569481460788     1.29671677868962
H  -6.97553277571059    -9.46756919425019     0.53582686950058
H  -1.99393602717009     0.93372698445531     0.00427411368887
H   4.16627046764179     0.09625024232982     1.83497833910662
C   3.21135803092747    -1.66793846353701     2.67143138560886
H   2.99047584362507     0.43245097496794     3.10750426784714
H   3.98448134765609    -1.82660804830526     3.43302647469580
H   3.47202033164796    -2.29911275049896     1.80835626154189
H   1.85127963479790    -3.15219049696549     3.48338710255360
H   1.61348515584753    -1.52077974984811     4.11605494284517
C  -2.96496525222738     3.55378819790922     2.36315782151057
H  -4.23527120841873     1.98989042935569     3.17459046375089
H  -3.77441409588430     1.75224306896423     1.49325472045285
H  -2.06664975377465     3.41712773547321     0.40417509514166
H  -1.42977360172432     4.73543162551962     1.38067615390860
H  -2.68882281427671     3.92355727507966     3.36130688158560
H  -3.79789281643679     4.17368231061681     2.00997557177020
```

References

1   A. Zagdoun, G. Casano, O. Ouari, M. Schwarzwälder, A. J. Rossini, F. Aussenac, M. Yulikov, G. Jeschke, C. Copéret, A. Lesage, P. Tordo and L. Emsley, Large Molecular Weight Nitroxide Biradicals Providing Efficient Dynamic Nuclear Polarization at Temperatures up to 200 K, *J. Am. Chem. Soc.*, 2013, **135**, 12790–12797.

2   G. M. Sheldrick, Crystal structure refinement with SHELXL, *Acta Crystallogr. Sect. C Struct. Chem.*, 2015, **71**, 3–8.

3   A. L. Spek, PLATON SQUEEZE: a tool for the calculation of the disordered solvent contribution to the calculated structure factors, *Acta Crystallogr. Sect. C Struct. Chem.*, 2015, **71**, 9–18.

4   S. Stoll and A. Schweiger, EasySpin, a comprehensive software package for spectral simulation and analysis in EPR, *J. Magn. Reson.*, 2006, **178**, 42–55.

5   S. Stoll and R. D. Britt, General and efficient simulation of pulse EPR spectra, *Phys. Chem. Chem. Phys.*, 2009, **11**, 6614.

6   S. Stoll, *CW-EPR Spectral Simulations: Solid State ☆*, Elsevier Inc., 2015, vol. 563.

7   F. Mentink-Vigier, S. Paul, D. Lee, A. Feintuch, S. Hediger, S. Vega and G. De Paëpe, Nuclear depolarization and absolute sensitivity in magic-angle spinning cross effect dynamic nuclear polarization, *Phys. Chem. Chem. Phys.*, 2015, **17**, 21824–21836.

8   R. Harrabi, T. Halbritter, F. Aussenac, O. Dakhlaoui, J. van Tol, K. K. Damodaran, D. Lee, S. Paul, S. Hediger, F. Mentink-Vigier, S. Th. Sigurdsson and G. De Paëpe, Highly Efficient Polarizing Agents for MAS-DNP of Proton-Dense Molecular Solids, *Angew. Chem. Int. Ed.*, 2022, **61**, e202114103.

9   Q. Chen, S. S. Hou and K. Schmidt-Rohr, A simple scheme for probehead background suppression in one-pulse 1H NMR, *Solid State Nucl. Magn. Reson.*, 2004, **26**, 11–15.

10 P. E. Kristiansen, M. Carravetta, W. C. Lai and M. H. Levitt, A robust pulse sequence for the determination of small homonuclear dipolar couplings in magic-angle spinning NMR, *Chem. Phys. Lett.*, 2004, **390**, 1–7.

11 P. E. Kristiansen, M. Carravetta, J. D. van Beek, W. C. Lai and M. H. Levitt, Theory and applications of supercycled symmetry-based recoupling sequences in solid-state nuclear magnetic resonance, *J. Chem. Phys.*, 2006, **124**, 234510.

12 K. Märker, S. Hediger and G. De Paëpe, Efficient 2D double-quantum solid-state NMR spectroscopy with large spectral widths, *Chem. Commun.*, 2017, **53**, 9155–9158.

13 M. Lee and W. I. Goldburg, Nuclear-Magnetic-Resonance Line Narrowing by a Rotating rf Field, *Phys. Rev.*, 1965, **140**, A1261–A1271.

14 B. M. Fung, A. K. Khitrin and K. Ermolaev, An Improved Broadband Decoupling Sequence for Liquid Crystals and Solids, *J. Magn. Reson.*, 2000, **142**, 97–101.

15 D. Lee, M. Wolska-Pietkiewicz, S. Badoni, A. Grala, J. Lewiński and G. De Paëpe, Disclosing Interfaces of ZnO Nanocrystals Using Dynamic Nuclear Polarization: Sol-Gel versus Organometallic Approach, *Angew. Chem. Int. Ed.*, 2019, **58**, 17163–17168.

16 M. Wolska-Pietkiewicz, A. Grala, I. Justyniak, D. Hryciuk, M. Jędrzejewska, J. Grzonka, K. J. Kurzydłowski and J. Lewiński, From Well-Defined Alkylzinc Phosphinates to Quantum-Sized ZnO Nanocrystals, *Chem. – Eur. J.*, 2017, **23**, 11856–11865.

17 K. R. Thurber and R. Tycko, Perturbation of nuclear spin polarizations in solid state NMR of nitroxide-doped samples by magic-angle spinning without microwaves, *J. Chem. Phys.*, 2014, **140**, 184201.

18 F. Mentink-Vigier, A.-L. Barra, J. van Tol, S. Hediger, D. Lee and G. De Paëpe, *De novo* prediction of cross-effect efficiency for magic angle spinning dynamic nuclear polarization, *Phys. Chem. Chem. Phys.*, 2019, **21**, 2166–2176.

19 F. Mentink-Vigier, Optimizing nitroxide biradicals for cross-effect MAS-DNP: the role of *g* -tensors' distance, *Phys. Chem. Chem. Phys.*, 2020, **22**, 3643–3652.

20 K. R. Thurber and R. Tycko, Theory for cross effect dynamic nuclear polarization under magic-angle spinning in solid state nuclear magnetic resonance: The importance of level crossings, *J. Chem. Phys.*, 2012, **137**, 084508.

21 F. Mentink-Vigier, Ü. Akbey, Y. Hovav, S. Vega, H. Oschkinat and A. Feintuch, Fast passage dynamic nuclear polarization on rotating solids, *J. Magn. Reson.*, 2012, **224**, 13–21.

22 F. Mentink-Vigier, S. Vega and G. De Paëpe, Fast and accurate MAS–DNP simulations of large spin ensembles, *Phys. Chem. Chem. Phys.*, 2017, **19**, 3506–3522.

23 F. Mentink-Vigier, T. Dubroca, J. Van Tol and S. Th. Sigurdsson, The distance between g-tensors of nitroxide biradicals governs MAS-DNP performance: The case of the bTurea family, *J. Magn. Reson.*, 2021, **329**, 107026.

24 M. Bak and N. C. Nielsen, REPULSION, A Novel Approach to Efficient Powder Averaging in Solid-State NMR, *J. Magn. Reson.*, 1997, **125**, 132–139.